NASA TN D-485

NASA TN D-485

TECHNICAL NOTE

D-485

A LOW-RESOLUTION UNCHOPPED RADIOMETER FOR SATELLITES

R. A. Hanel

Goddard Space Flight Center

NATIONAL AERONAUTICS AND SPACE ADMINISTRATION

WASHINGTON February 1961

D

A LOW-RESOLUTION UNCHOPPED RADIOMETER FOR SATELLITES

by
R. A. Hanel

SUMMARY

The blackbody temperature and the albedo of a planet, and the variation of both parameters with latitude, longitude, and time, are of great value in understanding the climatic and meteorological conditions of the planet. An unchopped radiometer with a wide but restricted field of view is capable of such temperature and albedo measurements. Coated thermistors mounted in highly reflective cones serve as detectors. Their performance as sensor elements is analyzed in detail herein to prove the feasibility of the measurement. The simplicity of the instrumentation and the low information bandwidth required make the experiment equally attractive for earth satellites and space probes.

CONTENTS

A LOW-RESOLUTION UNCHOPPED RADIOMETER FOR SATELLITES

INTRODUCTION

Measurement of the optical and thermal properties of the earth and other planets is one of the basic experiments that can be performed by means of satellites and space probes. Incoming and outgoing radiation determine the energy budget of a planet and are responsible for climate and weather in the broad sense. Measurements in narrow spectral bands can be used to determine atmospheric compositions and temperatures and to give information on surface conditions.

The goal in this field of research could be detailed maps of the planets, showing the visual picture, temperatures, and radiation in characteristic bands. All high-resolution maps obtainable by photography, television, and spot-scanning techniques require high rates of information transmission and, frequently, storage facilities in the probe. For many purposes, especially if overall global or planetary studies are involved, only average values over rather large areas (e.g., 300 by 300 miles) are of interest. Even in the case of earth satellites, where a high-resolution picture is possible, the relatively low information rate and the integrating property of the wide-field detector justify simultaneous measurements by devices with low and high resolution.

The simplest form of such a wide-field radiation measurement is the heat-balance experiment suggested by Suomi and Wexler in connection with the International Geophysical Year program (Reference 1). In this procedure the temperatures of small spheres, coated to discriminate between solar and terrestrial radiation, are sensed by thermistors. However, the omnidirectional device has restrictions in accuracy and resolution. It is especially desirable in an image-forming experiment to match the field of view of both high- and low-resolution instruments. Interesting correlations between cloud cover and radiation balance might be expected.

The main problem in such a simple, unchopped radiometer is the loss in sensitivity resulting from the restrictions in the field of view. A technique that overcomes this limitation is analyzed in this paper.

METHOD OF MEASUREMENT

In the suggested version a thermistor is mounted in the apex of a highly reflecting cone. The detector can be classified as a thermal detector cooled predominantly by radiation. Its temperature is governed by the equation of energy balance,

$$\varepsilon_t \sigma T_t^4 = k_1 \sigma T_e^4 + k_2 \sigma T_s^4 + k_2' 4\sigma T_0^3 (T_s - T_t) + k_3 A \mathscr{J} \sin \beta . \tag{1}$$

(All symbols are defined in Appendix A.)

Thermal radiation emitted by the thermistor balances radiation from the earth, radiation and heat conduction from the satellite, and finally the earth's reflected solar energy. The coefficients k consolidate optical as well as geometrical factors. The two unknowns, i.e., the blackbody temperature T_e and the albedo of the earth, can be determined if a second linearly independent equation is available.

In the experiment the second equation is provided by a second thermistor with different optical properties. One detector is coated black; it is equally sensitive to reflected sunlight and long-wave terrestrial radiation. The second detector is coated to be highly reflective in the visible and near infrared to about 3 microns (Reference 2). The surface appears white to the eye even though its emissivity in the infrared is very high. Since 99.9 percent of the terrestrial radiation is emitted at wavelengths longer than 4 microns, both detectors will show the same equilibrium temperature when they face the dark side of the earth. On the illuminated side the temperature of the black detector will rise — in contrast to that of the white one, which is hardly affected by reflected sunlight.

Careful measurement of the temperatures of both detectors and accurate calibration of all k values permits the determination of albedo and terrestrial radiation.* It has been tacitly assumed that the influence of the satellite temperature T_s can be kept small (k_2 and $k_2' \ll k_1$), or the thermistor would read essentially the satellite temperature. High thermal isolation of the detectors from the satellite structure is essential to the experiment, and the major part of this paper is devoted to that problem.

GEOMETRY OF THE CONE

The field of view of a thermistor mounted in a cone can best be visualized by utilizing the mirror image of the detector (Figure 1). The conical detector is equivalent to a

*This is exactly true only if radiation from the earth follows Lambert's cosine law; but since the atmosphere, with its peculiar absorption bands in the infrared and its temperature gradients, does not emit as a diffuse surface, certain corrections have to be made in the interpretation of data.

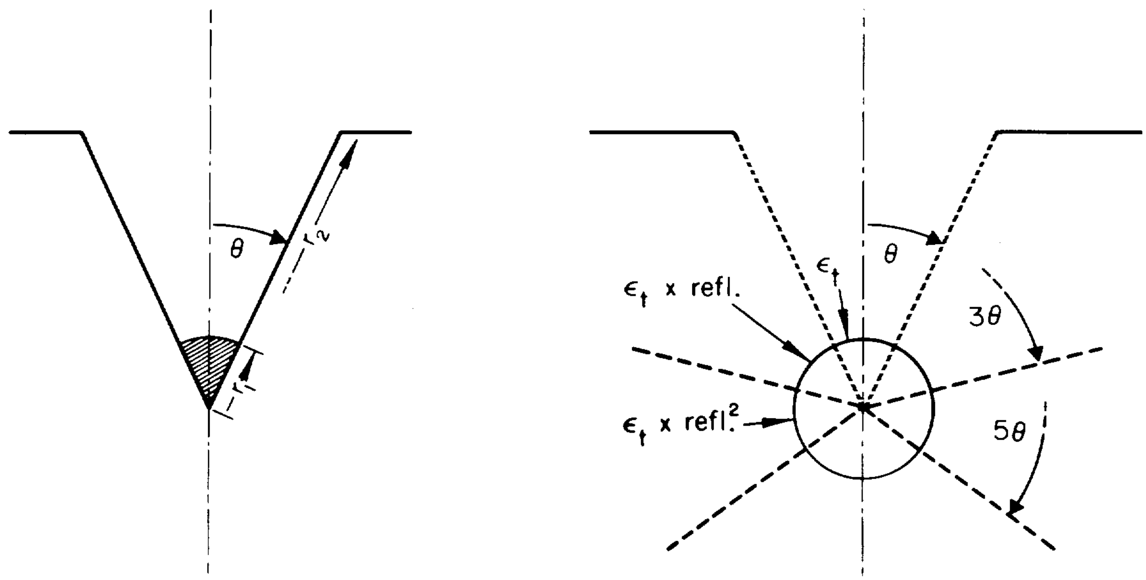

Figure 1 - Equivalent detector, imaging of thermistor

spherical one that is restricted in its field of view by an aperture equal to the base of the cone. Reflection losses could be taken into account by assuming a reduced emissivity for each image. It is justifiable to consider a sphere of uniform emissivity ε_t since evaporated metal surfaces have high (90-99 percent) reflectivity (Reference 3) and since only a few reflections are involved. Figure 2 shows the field of view for various thermistor-to-cone radius ratios r_1/r_2 and aperture angle θ.

The energy exchange is judged better by a second mode of imaging, that of imaging the source (Figure 3). The detector surface appears completely surrounded by the target. Radiation exchange between thermistor and earth is then described by

$$P = \varepsilon_t \sigma (T_e^4 - T_t^4)\, a_t \ . \qquad (2)$$

The term $a_t = 2\pi r_1^2 (1 - \cos\theta)$ represents the detector area. Without the conical reflector the same detector would receive approximately $P \sin^2\theta$. The gain introduced by the cone becomes about 5 for θ = 25 degrees. The same method of imaging permits estimation of the amount of radiation between cone and detector, as shown in Figure 4. Since the emissivity of the cone material can be kept as low as 0.02 and since a large portion of the cone will be at the satellite temperature, this effect — small to begin with — can be incorporated into the radiation exchange of the unexposed side of the thermistor mount.

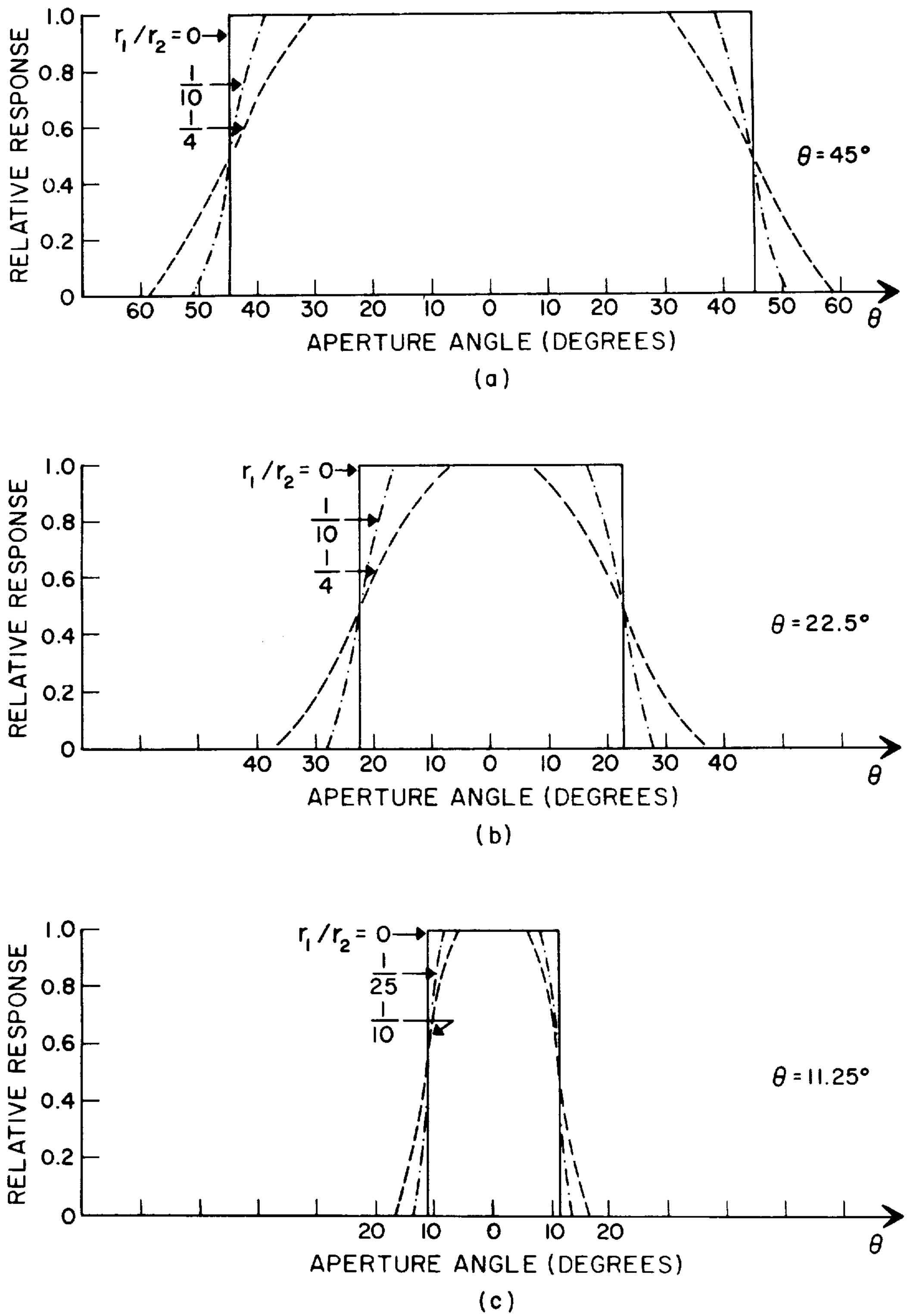

Figure 2 - Field of view of radiometer as a function of thermistor-to-cone radius ratio r_1/r_2 and aperture angle θ

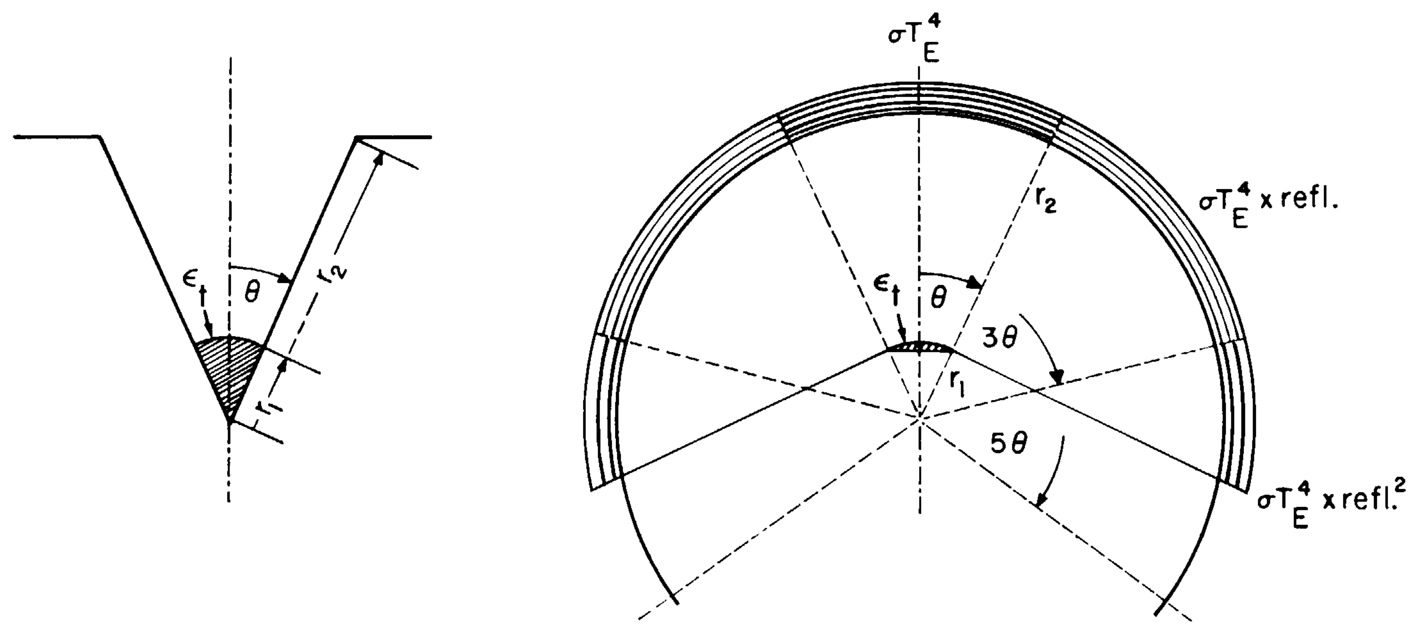

Figure 3 - Equivalent detector, imaging of radiation source

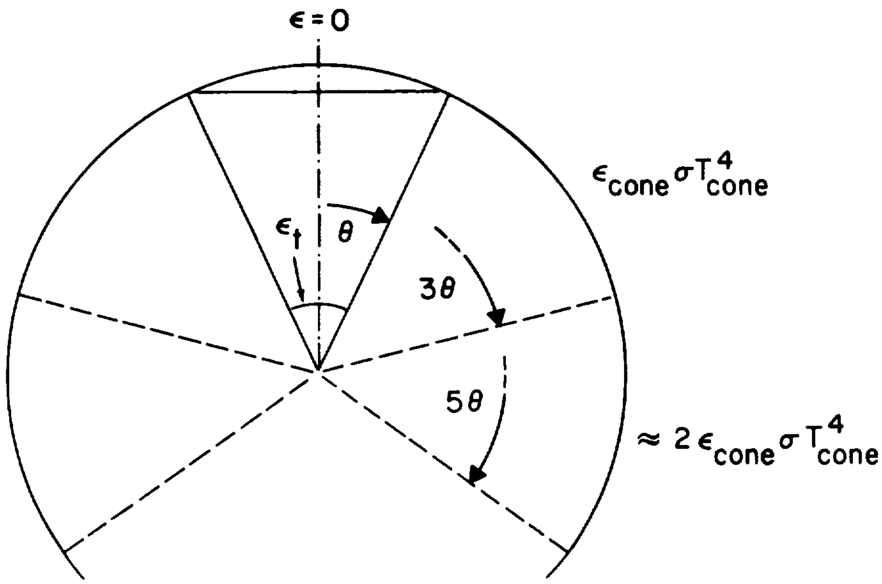

Figure 4 - Radiation exchange between cone and detector

RESOLUTION AND BANDWIDTH

The resolution of such a system and the electrical bandwidth required to transmit the gathered information are related to the altitude and speed of the vehicle. The detector, slowly scanning the earth as the satellite moves along, responds to the average radiation within its field of view (Figure 5). Any arbitrary intensity distribution in the scanning direction can be taken into consideration by superposition of periodic distributions of wavelength λ_n:

$$I_x = \sum_n a_n \exp\left(\frac{i2\pi x}{\lambda_n}\right). \tag{3}$$

The center x_0 of the field of view travels with subsatellite speed v_0 as the satellite, visualized as a stable platform, orbits around the earth. Consequently, x_0 is equal to vt; and, since

$$x = x_0 + r \cos \phi ,$$

the radiation received by the detector of radius r_1 from a solid angle Ω is given by

$$P_n = \int_\Omega r_1^2 a_n \exp(ik_n vt) \exp(ik_n r \cos \phi)\, d\Omega , \tag{4}$$

where k_n stands for $2\pi/\lambda_n$. The increment of the solid angle $d\Omega$ is derived from geometrical considerations:

$$d\Omega = \cos\theta \frac{r\,dr\,d\phi}{h^2 + r^2} . \tag{5}$$

Equation 4 can be integrated over ϕ by Sommerfeld's integral for Bessel functions (Reference 4):

$$P_n = \int_0^R 2\pi r_1^2 \alpha_n \exp(ikvt)\, h J_0(kr)(h^2 + r^2)^{-\frac{3}{2}} r^2\, dr . \tag{6}$$

This integral can be solved by partial integration:

$$P_n = \pi r_1^2 \alpha_n \exp(ikvt) \sum_{m=1}^{\infty} 2 \prod_{q=1}^{m} (2q - 1) \cos\theta \sin^{2m}\theta \frac{Jm(kR)}{(kR)^m} . \tag{7}$$

The first null in Equation 7 characterizes the resolving limit of the system. A small, square field of view exhibits a $\sin X/X$ characteristic and shows the first null at $X_1 = \pi$. A small, circular field of view has a $2J_1(X)/X$ scanning function, and the first null is at $X_1 = 3.8$. Evaluation of the sum in Equation 7 yields $X_1 = 4$; an altitude of 300 miles and an angle θ of 25 degrees were assumed. The wavelength λ, which corresponds to the first null, is then

$$\lambda_0 = \frac{2\pi R}{4} . \tag{8}$$

The corresponding electrical frequency band is given by Equation 9 (when v = 4.4 miles per second, and R = 140 miles):

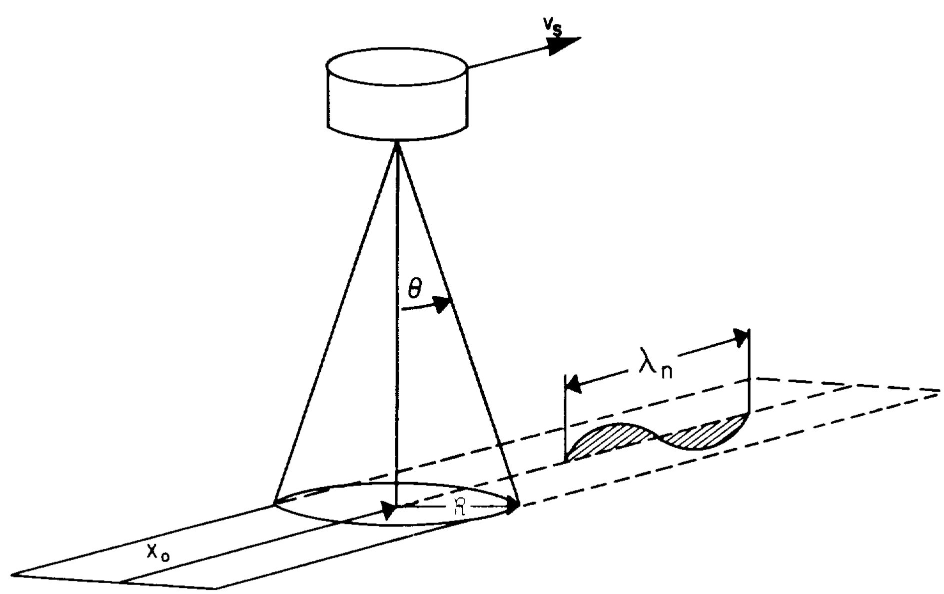

Figure 5 - Detector slowly scans earth as satellite moves along vector v_s

$$f_{max} = \frac{4v_0}{2\pi R} = 0.02 \text{ cps}. \tag{9}$$

The thermal time constant of the detector has to be chosen to accommodate to the highest frequency. Compared with those of other detection systems, these bandwidth requirements are very low.

ENERGY TRANSFER WITHIN THE CONE

A cross section of the detector assembly (Figure 6) shows the thermistor imbedded in the central area on the tip of the cone. The thermistor material could be deposited directly on the lower inner part of the Mylar cone. For small angles θ the black detector, being truly gray since its emissivity is about 0.8, would resemble an ideal blackbody. This procedure is not too advisable for the white detector, since the reflectivity for visible light is also reduced. The cover plate that shields the cone or cones from the interior of the satellite is made highly reflective ($\varepsilon = 0.02$). However, in the calculations an emissivity of 1 ($\varepsilon_s = 1$) was assumed. This seems to be justified for the following reasons.

Because of multi-reflections, the effective emissivity of two parallel surfaces of emissivity ε_1 and ε_2 facing each other is

$$\varepsilon_{eff} = \frac{\varepsilon_1 \varepsilon_2}{\varepsilon_1 + \varepsilon_2 - \varepsilon_1 \varepsilon_2} . \tag{10}$$

If both emissivities ε_1 and ε_2 are small and equal, ε_{eff} becomes $\varepsilon/2$. However, if radiation emitted by the rear surface of the thermistor is not reflected back to the detector but bounces back and forth between cone and cover plate until finally absorbed, then the cavity between cone and cover acts like a blackbody independent of wall emissivity, and ε_{eff} becomes equal to ε rather than to $\varepsilon/2$. The actual physical structure will be somewhere between these two cases, probably closer to the black cave model. Therefore, for the purpose of this calculation, and also to incorporate a small amount of radiation from the front surface of the detector to the outer areas of the cone, an emissivity of 1 was chosen for the cover plate.

The energy flux $Q(r)$ in the cone material is proportional to the temperature gradient,

$$Q(r) = -cD\, 2\pi r \sin\theta \frac{dT(y)}{dr} . \tag{11}$$

Simultaneously, $Q(r)$ is the flux into the cone tip plus the received or emitted radiation:

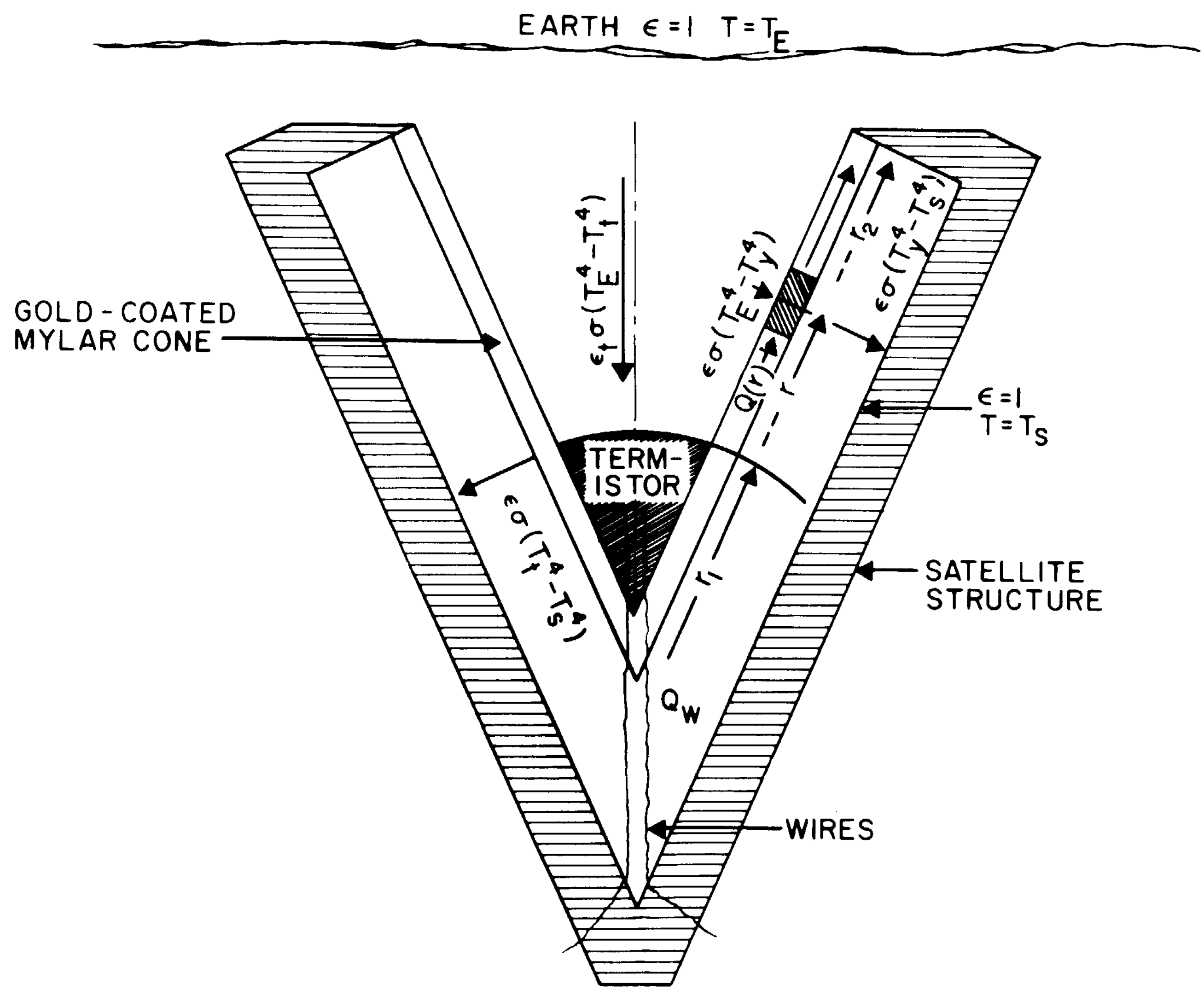

Figure 6 - Energy transfer within conical detector

$$Q(r) = Q(r_1) + \int_{r_1}^{r} \varepsilon\sigma\left(T_e^4 - T_y^4\right) da - \int_{r_1}^{r} \varepsilon\sigma\left(T_y^4 - T_s^4\right) da. \qquad (12)$$

The balance between incoming and outgoing radiation of the thermistor is

$$Q(r_1) = \epsilon_t\sigma(T_e^4 - T_t^4)\, 2\pi r_1^2 (1 - \cos\theta) - \int_0^{r_1} \varepsilon\sigma(T_t^4 - T_s^4)\, da - \frac{2c_w q_w (T_s - T_t)}{\ell}. \qquad (13)$$

These equations can be solved, after linearization by means of a reference temperature T_0:

$$\begin{aligned} T_y &= T_0 + y & T_y^4 &= T_0^4 + 4T_0^3 y + \cdots \\ T_t &= T_0 + t & T_t^4 &= T_0^4 + 4T_0^3 t + \cdots \\ T_s &= T_0 + S & T_s^4 &= T_0^4 + 4T_0^3 S + \cdots \\ T_e &= T_0 + E & T_e^4 &= T_0^4 + 4T_0^3 E + \cdots . \end{aligned} \qquad (14)$$

The error introduced by the omission of second-order terms can be kept small if T_0 is chosen close to the mid-range value of the temperatures involved. Furthermore, without loss in generality, the satellite temperature S can be taken equal to unity and the equivalent earth temperature equal to minus unity. Equations 11 through 13 then become

$$Q(r) = -cD\, 2\pi r \sin\theta \frac{dy}{dr}, \qquad (15)$$

$$Q(r) = Q(r_1) - 2\varepsilon\sigma 2\pi \sin\theta\, 4T_0^3 \int_{r_1}^{r} y\, r\, dr, \qquad (16)$$

$$Q(r_1) = \sigma 4T_0^3 \pi r_1^2 \left[-\varepsilon_t 2(1 - \cos\theta)(1 + t) + \varepsilon(1 - t)\sin\theta\right] + \frac{2c_w q_w (1 - t)}{\ell}. \qquad (17)$$

Differentiation of Equations 15 and 16 leads to a Bessel differential equation:

$$y'' + \frac{1}{r} y' - \frac{2\varepsilon\sigma 4T_0^3}{cD} y = 0, \qquad (18)$$

which is solved by Bessel and Hankel functions of order zero and imaginary argument (Reference 5),

$$y = aJ_0(i\xi r) + bH_0^{(1)}(i\xi r). \qquad (19)$$

The parameter ξ is introduced for brevity:

$$\xi^2 = 2\,\frac{4\varepsilon\sigma T_0^3}{cD}\,. \tag{20}$$

Boundary conditions determine the constants a and b in Equation 19. One boundary condition states that the temperature of the base of the cone must be the satellite temperature:

$$y(r = r_2) = +1\,. \tag{21}$$

The introduction of Equation 21 into Equation 19 yields

$$y = \frac{H_0(i\xi r)}{H_{02}} + \frac{a\left[J_0(i\xi r)H_{02} - J_{02}H_0(i\xi r)\right]}{H_{02}}\,. \tag{22}$$

At the other boundary $r = r_1$, the thermal flux must be $Q(r_1)$ as specified by Equation 17, which determines the remaining constant a:

$$a = \frac{\dfrac{\xi r_1}{4\varepsilon\,\sin\theta}\left[\varepsilon(\rho + \sin\theta)\left(1 - \dfrac{H_{01}}{H_{02}}\right) - \varepsilon_t 2(1 - \cos\theta)\left(1 + \dfrac{H_{01}}{H_{02}}\right)\right] - i\,\dfrac{H_{11}}{H_{02}}}{\dfrac{\xi r_1}{4\varepsilon\,\sin\theta}\left[\varepsilon(\rho + \sin\theta) + \varepsilon_t 2(1 - \cos\theta)\right](J_{01}H_{02} - J_{02}H_{01}) + i(J_{11}H_{02} - J_{02}H_{01})}\,. \tag{23}$$

In Equation 23, ρ stands for

$$\rho = \frac{c_w q_w}{\ell\varepsilon\sigma\,4T_0^3\,\pi r_1^2}\,. \tag{24}$$

Since the general solution for y equals t for $r = r_1$, the thermistor temperature is given by

$$t = \frac{H_{01}}{H_{02}} + \frac{a(J_{01}H_{02} - J_{02}H_{01})}{H_{02}}\,; \tag{25}$$

and finally, by substitution of a and rearrangement of terms,

$$t = \frac{\dfrac{\varepsilon(\rho + \sin\theta) - \varepsilon_t 2(1 - \cos\theta)}{4\varepsilon\,\sin\theta} + \dfrac{i}{\xi r_1}\,\dfrac{J_{11}H_{01} - J_{01}H_{11}}{J_{01}H_{02} - J_{02}H_{01}}}{\dfrac{\varepsilon(\rho + \sin\theta) + \varepsilon_t 2(1 - \cos\theta)}{4\varepsilon\,\sin\theta} + \dfrac{i}{\xi r_1}\,\dfrac{J_{11}H_{02} - J_{02}H_{11}}{J_{01}H_{02} - J_{02}H_{01}}}\,. \tag{26}$$

Figure 7 shows the thermistor temperature t expressed by this equation (using numerical values from Reference 4). The thermistor temperature is within the two limits: the satellite temperature $S = +1$, and the earth temperature $E = -1$. A variety of parameters consolidated in x_1 and x_2 determines t. The abscissa in Figure 7 is x_1, and the curves correspond to a particular value of x_2. The parameters x_1 and x_2 are

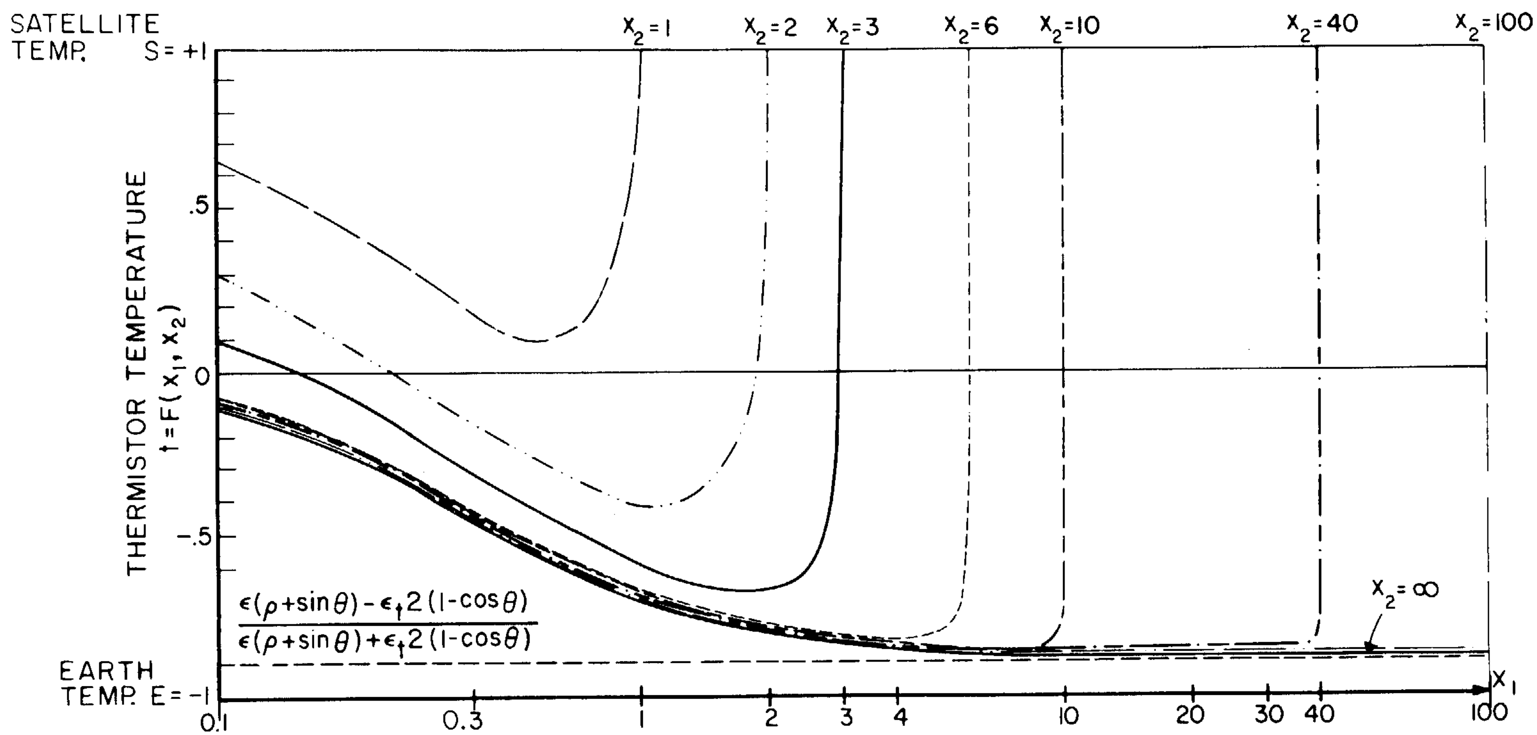

$\epsilon_t = 0.8, \epsilon = 0.02; \rho = 0; \theta = 26°$

Figure 7 - Thermistor temperature as a function of $x_1 = r_1\sqrt{\frac{2\epsilon\sigma 4T_0^3}{cD}}$ and $x_2 = r_2\sqrt{\frac{2\epsilon\sigma 4T_0^3}{cD}}$

proportional to the dimensions of the thermistor, r_1, and of the cone, r_2. They should be chosen so that t approaches the earth temperature E as closely as possible without unnecessarily increasing the physical dimensions of the detector. The value $x_1 = 3$ seems to be a good compromise. For thermal reasons alone, $x_2 \geq 6$ would be sufficient; however, a well defined field of view requires $x_2 \geq 4x_1$. The radii r_1 and r_2 can then be determined:

$$r_1 = x_1 \sqrt{\frac{cD}{2\varepsilon\sigma 4 T_0^3}} ; \qquad r_2 = x_2 \sqrt{\frac{cD}{2\varepsilon\sigma 4 T_0^3}} . \tag{27}$$

Numerical values for a 1-mil gold-coated Mylar cone yield a thermistor size of about 1 square centimeter, a reasonable dimension.

To this point, the influence of wires connecting the thermistor electrically to the resistance-measuring instrument has been neglected. This is justified, as can be seen from Equation 26, as long as $\rho < \sin\theta$ or $c_w q_w < \ell\sigma 4 T_0^3 \pi r_1^2 \sin\theta$, a condition that can easily be met by a thin platinum wire (gage number 30, $\ell = r_2$).. Heat conduction through the wires can therefore be neglected.

CALIBRATION OF THE INSTRUMENT

A very important task will be the determination of the coefficients k. The linearized form of Equation 1 for both the black and the white thermistors yields two equations:

$$t_{bl} = k_{11}E + k_{12}S + k_{13}A ,$$

$$t_w = k_{21}E + k_{22}S + k_{23}A . \tag{28}$$

The constants k_{11}, k_{13}, and k_{21} will be chosen high, perhaps 0.9. By proper coating, the residual responsivity of the white detector to sunlight k_{23} will be made as small as possible. Calculations in this paper have shown that the combined effect of radiation and conduction from the satellite structure, k_{12} and k_{22}, can be made very small indeed (0.1). The experimental verification and determination of all k's is the most important part of the calibration. The temperatures of the black and the white thermistors and the satellite structure will be telemetered back to earth; then Equation 28 can be solved for the unknowns: the blackbody temperature E and the reflected solar energy A.

ACKNOWLEDGMENTS

The author wishes to thank Mr. W. G. Stroud of the Goddard Space Flight Center, for his constant encouragement and Dr. V. Suomi of the University of Wisconsin, for many discussions on the subject. Mr. R. De Waard and Mr. E. A. Jackson of the Barnes Engineering Company are presently constructing an experimental model. Messrs. R. Carter, C. Catoe, and R. Wiack, of the GSFC, performed calibration tests; and most of the numerical calculations have been carried out by Mr. J. Fedor, also of GSFC.

REFERENCES

1. Suomi, V. E., "A Proposal for Obtaining the Radiation Balance of the Earth from a Satellite," National Academy of Sciences, U. S. National Committee for the International Geophysical Year, October 17, 1956
2. Reid, C. D., and McAlister, E. D., "Measurement of Spectral Emissivity from 2μ to 15μ," J. Opt. Soc. Amer. 49(1):78-82, January 1959
3. "Reflection of Light on Metals," Handbook of Chemistry and Physics, 41st ed. Cleveland: Chemical Rubber Publishing Company, 1960, pp. 2945-2950
4. Jahnke, E. and Emde, F., "Tables of Functions with Formulae and Curves," New York: Dover Publications, 1943
5. McLachlan, N. W., "Bessel Functions for Engineers," 2nd ed., Oxford: Clarendon Press, 1955

Appendix A

LIST OF SYMBOLS

A	albedo
a_t	detector area
a, b, α, k	constants
c	specific conductivity
c_w	specific conductivity of connecting wire
D	thickness of cone material
da	areal element
E	temperature of earth relative to reference temperature
f	frequency
$H_m^{(1)}(i\xi r)$	Hankel's function of first kind, m^{th} order of the argument $(i\xi r)$
H_{01}	$H_0^{(1)}(i\xi r_1)$
H_{02}	$H_0^{(1)}(i\xi r_2)$
H_{11}	$H_1^{(1)}(i\xi r_1)$
h	satellite altitude
I	intensity
$J_m(i\xi r)$	Bessel's function of m^{th} order of the argument $(i\xi r)$
J_{01}	$J_0(i\xi r_1)$
J_{02}	$J_0(i\xi r_2)$
J_{11}	$J_1(i\xi r_1)$
$k_n = \frac{2\pi}{\lambda_n}$	wave number
ℓ	length of connecting wire
P	total radiant flux
Q(r)	thermal flux in cone
q_w	cross section of connecting wire
q, m, n	indices of summation

$\mathcal{R}$ radius of target area

$\mathcal{r}$ radius to arbitrary point in the target area

r_1 radius of thermistor

r_2 radius of cone

r radius to an arbitrary point of the cone

S temperature of structure of satellite relative to reference temperature

$\mathcal{S}$ solar constant

T absolute temperature (°K)

T_e equivalent temperature of earth

T_o reference temperature

T_s temperature of mounting structure

T_t temperature of thermistor

T_y temperature of cone material

t temperature of thermistor relative to reference temperature

$\mathcal{t}$ time

v subsatellite speed

X_1 first zero $F(X_1) = 0$

x subsatellite path; arbitrary variable

x_0 center of field of view

x_1 auxiliary parameter (see Figure 7)

x_2 auxiliary parameter (see Figure 7)

y temperature of cone relative to reference temperature

β elevation angle

ε emissivity of cone surface (= 0.02)

ε_s emissivity of mounting structure in satellite (= 1)

ε_t emissivity of thermistor (= 0.8)

λ_n wavelength of intensity distribution (Figure 5)

Ω solid angle

ϕ azimuth angle

ρ $c_w q_w / \ell \varepsilon \sigma 4 T_0^3 \pi r_1^2$ as defined by Equation 24

σ Stefan-Boltzmann radiation constant

θ aperture angle (one-half of field of view)

ξ $\sqrt{2\varepsilon\sigma 4T_0^3/cD}$ as defined by Equation 20

NASA - Langley Field, Va.

NASA TN D-485
National Aeronautics and Space Administration.
A LOW-RESOLUTION UNCHOPPED RADIOMETER FOR SATELLITES. R. A. Hanel. February 1961. 16p. OTS price, $0.50.
(NASA TECHNICAL NOTE D-485)

The black-body temperature and the albedo of a planet, and the variation of both parameters with latitude, longitude, and time, are of great value in understanding the climatic and meteorological conditions of the planet. An unchopped radiometer with a wide but restricted field of view is capable of such temperature and albedo measurements. Coated thermistors mounted in highly reflective cones serve as detectors. Their performance as sensor elements is analyzed in detail herein to prove the feasibility of the measurement. The simplicity of the instrumentation and the low information bandwidth required make the experiment equally attractive for earth satellites and space probes.

Copies obtainable from NASA, Washington

I. Hanel, Rudolf A.
II. NASA TN D-485

(Initial NASA distribution:
7, Astrophysics; 17, Communications and sensing equipment, flight;
21, Geophysics and geodesy;
47, Satellites.)

NASA

NASA TN D-485
National Aeronautics and Space Administration.
A LOW-RESOLUTION UNCHOPPED RADIOMETER FOR SATELLITES. R. A. Hanel. February 1961. 16p. OTS price, $0.50.
(NASA TECHNICAL NOTE D-485)

The black-body temperature and the albedo of a planet, and the variation of both parameters with latitude, longitude, and time, are of great value in understanding the climatic and meteorological conditions of the planet. An unchopped radiometer with a wide but restricted field of view is capable of such temperature and albedo measurements. Coated thermistors mounted in highly reflective cones serve as detectors. Their performance as sensor elements is analyzed in detail herein to prove the feasibility of the measurement. The simplicity of the instrumentation and the low information bandwidth required make the experiment equally attractive for earth satellites and space probes.

Copies obtainable from NASA, Washington

I. Hanel, Rudolf A.
II. NASA TN D-485

(Initial NASA distribution:
7, Astrophysics; 17, Communications and sensing equipment, flight;
21, Geophysics and geodesy;
47, Satellites.)

NASA

NASA TN D-485
National Aeronautics and Space Administration.
A LOW-RESOLUTION UNCHOPPED RADIOMETER FOR SATELLITES. R. A. Hanel. February 1961. 16p. OTS price, $0.50.
(NASA TECHNICAL NOTE D-485)

The black-body temperature and the albedo of a planet, and the variation of both parameters with latitude, longitude, and time, are of great value in understanding the climatic and meteorological conditions of the planet. An unchopped radiometer with a wide but restricted field of view is capable of such temperature and albedo measurements. Coated thermistors mounted in highly reflective cones serve as detectors. Their performance as sensor elements is analyzed in detail herein to prove the feasibility of the measurement. The simplicity of the instrumentation and the low information bandwidth required make the experiment equally attractive for earth satellites and space probes.

Copies obtainable from NASA, Washington

I. Hanel, Rudolf A.
II. NASA TN D-485

(Initial NASA distribution:
7, Astrophysics; 17, Communications and sensing equipment, flight;
21, Geophysics and geodesy;
47, Satellites.)

NASA

NASA TN D-485
National Aeronautics and Space Administration.
A LOW-RESOLUTION UNCHOPPED RADIOMETER FOR SATELLITES. R. A. Hanel. February 1961. 16p. OTS price, $0.50.
(NASA TECHNICAL NOTE D-485)

The black-body temperature and the albedo of a planet, and the variation of both parameters with latitude, longitude, and time, are of great value in understanding the climatic and meteorological conditions of the planet. An unchopped radiometer with a wide but restricted field of view is capable of such temperature and albedo measurements. Coated thermistors mounted in highly reflective cones serve as detectors. Their performance as sensor elements is analyzed in detail herein to prove the feasibility of the measurement. The simplicity of the instrumentation and the low information bandwidth required make the experiment equally attractive for earth satellites and space probes.

Copies obtainable from NASA, Washington

I. Hanel, Rudolf A.
II. NASA TN D-485

(Initial NASA distribution:
7, Astrophysics; 17, Communications and sensing equipment, flight;
21, Geophysics and geodesy;
47, Satellites.)

NASA